nature materials

LETTERS

PUBLISHED ONLINE: 15 DECEMBER 2013 | DOI: 10.1038/NMAT3836

Giant frictional dissipation peaks and charge-density-wave slips at the $NbSe_2$ surface

Markus Langer[1], Marcin Kisiel[1]*, Rémy Pawlak[1], Franco Pellegrini[2,3], Giuseppe E. Santoro[2,3,4], Renato Buzio[5], Andrea Gerbi[5], Geetha Balakrishnan[6], Alexis Baratoff[1], Erio Tosatti[2,3,4] and Ernst Meyer[1]

Understanding nanoscale friction and dissipation is central to nanotechnology[1–4]. The recent detection of the electronic-friction drop caused by the onset of superconductivity in Nb (ref. 5) by means of an ultrasensitive non-contact pendulum atomic force microscope (AFM) raised hopes that a wider variety of mechanical-dissipation mechanisms become accessible. Here, we report a multiplet of AFM dissipation peaks arising a few nanometres above the surface of $NbSe_2$—a layered compound exhibiting an incommensurate charge-density wave (CDW). Each peak appears at a well-defined tip–surface interaction force of the order of a nanonewton, and persists up to 70 K, where the short-range order of CDWs is known to disappear. Comparison of the measurements with a theoretical model suggests that the peaks are associated with local, tip-induced 2π phase slips of the CDW, and that dissipation maxima arise from hysteretic behaviour of the CDW phase as the tip oscillates at specific distances where sharp local slips occur.

Bodies in relative motion separated by large vacuum gaps of one or more nanometres experience a tiny frictional force, whose nature is now beginning to be accessible[6]. Measuring these minute frictional forces, and relating them to the underlying physics and collective phenomena of electrons, ions, spins and their phase transitions represents a challenging and valuable prospective form of local spectroscopy of the solid surface under the tip. Although extremely delicate, this non-contact form of friction is now measurable by a highly sensitive AFM cantilever oscillating like a pendulum over the surface[5,7,8]. The pendulum configuration takes advantage of very small spring constants, typically of the order of millinewtons per metre. The corresponding minimal detectable non-contact friction is extremely small, about $\Gamma_0^{\mathrm{pend}} \sim 10^{-12}\,\mathrm{kg\,s^{-1}}$, compared with $\Gamma_0^{\mathrm{TF}} \sim 10^{-7}\,\mathrm{kg\,s^{-1}}$ of more conventional tuning-fork tips (Methods), which work at smaller distances, just outside the repulsive regime. Here we use the pendulum to demonstrate a new example of non-contact friction, occurring when the vibrating tip pumps integer 2π slips onto the local surface phase of a CDW.

Layered dichalchogenides have long been known for their phase transitions leading to picometre-sized superstructure lattice distortions and corresponding new electronic periodicities in their low-temperature ground state[9]. Among them, $NbSe_2$ (with 2H stacking) stands out as a material exhibiting bulk CDW below the long-range-order onset temperature $T_{\mathrm{CDW}} = 33\,\mathrm{K}$ (ref. 10), as well as superconductivity below $T = 7.2\,\mathrm{K}$. The CDW consists of a joint periodic lattice distortion and electron density modulation, with the same incommensurate periodicity close to (3×3) in the layer plane, and a remarkably coherent phase, extending over hundreds of lattice spacings in clean samples. Whereas in other isoelectronic compounds of that family, such as TaS_2 (with 1T stacking), the CDW has a clear connection with the Fermi surface, thus leading to an insulating or near-insulating state at low temperatures[9], the driving force in $NbSe_2$ is now known to be different, not directly involving the Fermi surface, as recently ascertained both experimentally[11–15] and theoretically[14]. The distortion of $NbSe_2$ is thus really only a periodic lattice distortion. Nonetheless, we stick to the commonly used term CDW to avoid language confusion.

We measured the friction force acting between an *in situ* cleaved $NbSe_2$ surface and a sharp silicon cantilever tip oscillating in the pendulum geometry as well as a qPlus tuning-fork tip. We simultaneously acquired the tip oscillation frequency f and a dissipation signal P under ultrahigh-vacuum (UHV) conditions and low temperatures of $T = 5$–$6\,\mathrm{K}$, at which CDW and superconductivity coexist. As a function of tip–surface distance, we observed a remarkable train of dissipation maxima that extend as far out as a few nanometres above the surface. To understand their origin we consider a theoretical model, where the CDW is treated as an elastic medium coupled to the spatially extended oscillating cantilever tip (Fig. 1a). A comparison of AFM data with theory allows us to conclude that the series of dissipation maxima is due to a hysteretic behaviour of the CDW phase as the tip oscillates at specific distances where sharp local slips occur.

We first obtained, by means of a standard tuning-fork scanning tunnelling microscope (STM), the atomically resolved surface topography showing the additional CDW induced Moiré pattern as shown in Fig. 1b. The CDW modulation is incommensurate with the underlying lattice, as is well known[10,16]. Depending on the chosen spot, the CDW modulation is known to exhibit its incommensurate deviation from the nearby (3×3) commensurate periodicity either along one, or simultaneously along all three, planar directions[17]. In the proximity of the few visible surface defects (CO adsorbates and Se vacancies) the CDW distortion, pinned by the impurity, survives well above the pristine T_{CDW}.

In Fig. 1c the non-contact friction $P(z, V)$ versus tip–sample distance z and tip–sample voltage V as the tip approaches the sample surface is shown for the pendulum AFM. The dissipated

[1]Department of Physics, University of Basel, Klingelbergstraße 82, Basel 4056, Switzerland, [2]SISSA, Via Bonomea 265, Trieste 34136, Italy, [3]CNR-IOM Democritos National Simulation Center, Via Bonomea 265, Trieste I-34136, Italy, [4]International Centre for Theoretical Physics (ICTP), PO Box 586, Trieste I-34014, Italy, [5]CNR-SPIN Institute for Superconductivity, Innovative Materials and Devices, C.so Perrone 24, Genova 16152, Italy, [6]Department of Physics, University of Warwick, Coventry CV4 7AL, UK. *e-mail: marcin.kisiel@unibas.ch

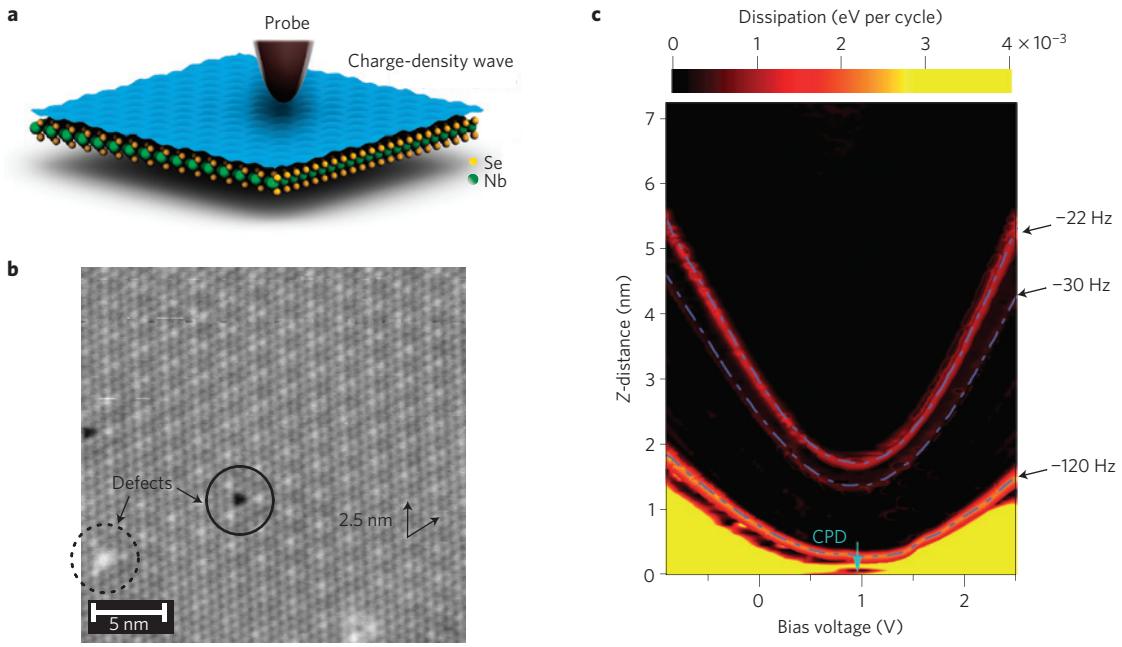

Figure 1 | Observation of a charge-density wave on a $NbSe_2$ surface and accompanied non-contact friction. a, An oscillating AFM tip in proximity to the charge-density wave on the $NbSe_2$ surface. **b**, Constant-current STM ($I = 10$ pA, $V = 5$ mV) image of the $NbSe_2$ surface showing a hexagonal CDW-induced Moiré pattern as well as two types of surface defect—adsorbed CO molecules (dashed circle) and Se atom vacancies (solid circle). **c**, Energy dissipation between the $NbSe_2$ surface and the pendulum-AFM tip versus tip-sample distance (Z) and bias voltage V. Bright features on the image represent large non-contact friction. Friction increase is at the same cantilever frequency $f = f_0 - 22$ Hz, $f = f_0 - 30$ Hz, $f = f_0 - 120$ Hz, and the constant frequency contours are shown with dashed lines. The distance $d = 0$ corresponds to the point where the tip enters the contact regime, which we clearly see in the cantilever deflection signal. Measurements were acquired at $T = 6$ K.

power in units of electronvolts per cycle is calculated according to a standard formula, measuring the difference between the power in (first term) and out (second term) of the tip[18]:

$$P = P_0\left(\frac{A_{\mathrm{exc}}(d)}{A_{\mathrm{exc},0}} - \frac{f(d)}{f_0}\right) \quad (1)$$

where P_0 is the dissipated power due to intrinsic losses of the cantilever, measured at large tip–sample separation, $A_{\mathrm{exc}}(d)$ and $f(d)$ are the distance-dependent excitation amplitude (as measured by the excitation voltage needed to excite the cantilever at constant oscillation amplitude A) and frequency of the cantilever, respectively, and the suffix zero refers to the free cantilever. In the case of pendulum AFM, the frequency and the amplitude of lateral oscillations are equal to $f_0 = 12$ kHz and $A = 5$ nm, respectively. Owing to the tip asymmetry (Methods and Supplementary Fig. 1), there is a non-negligible perpendicular oscillation amplitude $A_{\mathrm{perp}} = 180$ pm as well. Bright features on Fig. 1c correspond to high dissipation maxima up to $P = 2$ meV per cycle observed already at some nanometres above the sample surface. Within each dissipation branch, the amount of energy loss stays constant, independently of the bias voltage V. The giant non-contact friction maxima remain well defined even after careful compensation of the contact potential difference (CPD) between the tip and the sample. The peaks persist whether the tip–surface interaction force F is van der Waals ($V = V_{\mathrm{CPD}} = +0.95$ V) or electrostatic ($V \neq V_{\mathrm{CPD}}$). Moreover, the $z(V)$ voltage dependence of each dissipation branch has a parabolic behaviour (as expected for an electrostatic capacitive interaction between a roughly conical tip and sample, where $F \sim V^2/d$), implying that each dissipation maximum always occurs at the same tip–surface interaction force as the voltage changes. Thus, the effect is force-controlled rather than voltage-controlled.

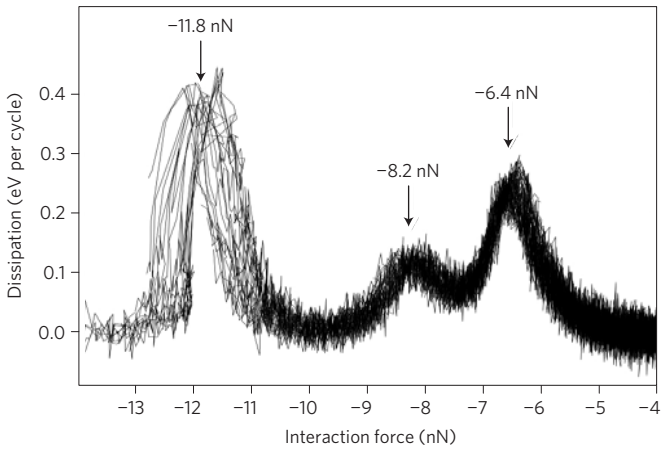

Figure 2 | Energy dissipation versus tip–sample interaction force F_{int}. Several spectra for different bias voltages V applied between the tuning-fork tip and the $NbSe_2$ surface are superimposed. Three dissipation maxima appear always at the same F_{int}, independent of V. Measurements were acquired at $T = 5$ K.

So far we have presented the pendulum-AFM results. To further confirm and ascertain the universal nature of this new effect, we repeat the experiment on an alternative instrument, the tuning-fork AFM. In this set-up, the tip oscillation direction is perpendicular to the sample surface, making the measurement more localized and ultimately more consistent across the surface. Figure 2 shows the non-contact friction of this different probe, again as a function of V (-0.4 V $< V < 1.5$ V), and the dissipated power again calculated according to equation (1), where $f_0 = 25$ kHz and $A = 200$ pm. Tuning-fork results systematically show three

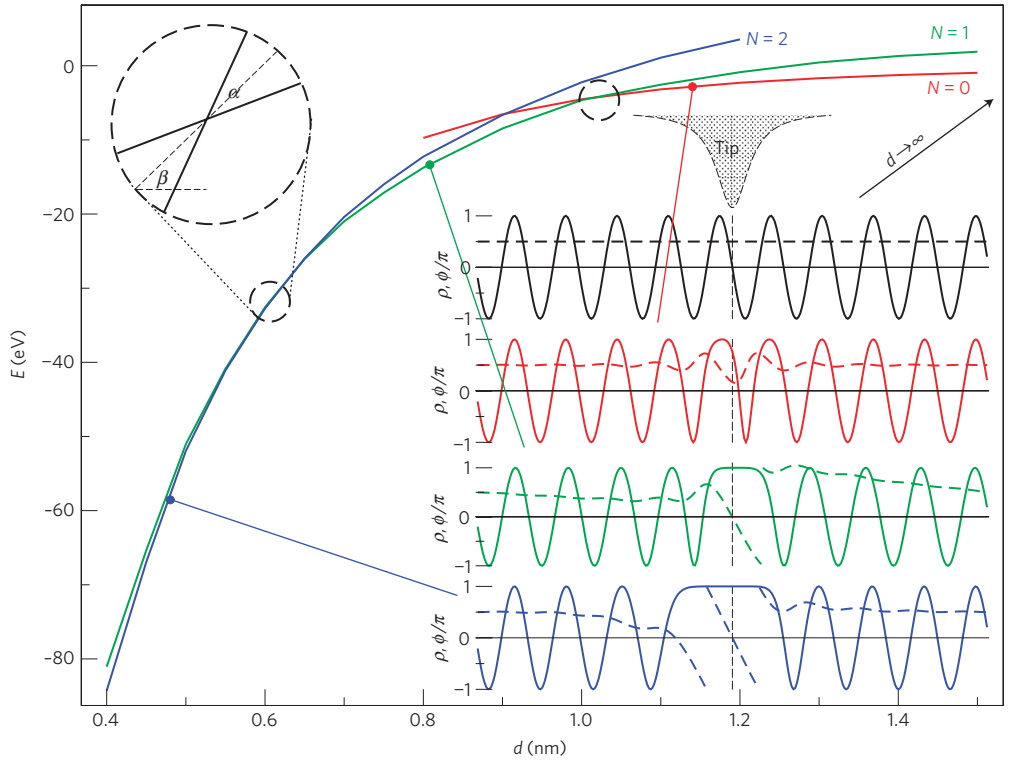

Figure 3 | Energy as a function of distance *d* for the elastic CDW model under the tip perturbation. Solutions are reported for different winding numbers *N*. The dashed circles represent the crossover points. Inset: charge density ρ (full lines) and phase ϕ (dashed lines; see equation (2)) along the CDW direction for (from top to bottom) no perturbation and increasing perturbations with winding number $N = 0, 1$ and 2 (at the marked distances *d*). The charge oscillation wavelength is $2\pi/Q$ and the position of the tip is indicated by the dashed vertical line. The ϕ boundary conditions are fixed at $\pi/2$.

reproducible dissipation maxima positioned at different interaction forces $F_{\mathrm{int}} = -6.4\,\mathrm{nN}$, $-8.2\,\mathrm{nN}$, $-11.8\,\mathrm{nN}$ as the tip approaches the surface (distance $0\,\mathrm{nm} < d < 2\,\mathrm{nm}$, and the attractive force was extracted from the cantilever frequency data by means of the Sader–Jarvis algorithm[19]). The finding of sharp dissipation peaks, a single one of which was already reported[20], is contrary to most non-contact friction experiments, where the energy dissipation P increases smoothly as the interaction force rises[5–8]. In particular, tip dissipation on a NbS_2 sample, yet another layered dichalcogenide compound, but without CDW, shows only a smooth increase (see Supplementary Fig. 3). In summary, two independent UHV experiments—the pendulum AFM (Fig. 1c) and, with much smaller intensity, the tuning-fork AFM (Fig. 2)—find a sequence of dissipation peaks extending as far out as several nanometres above the surface.

What is their origin? Even before any theory, temperature provides a suggestion that the dissipation peaks are related to the coupling of the tip to the CDW distortion. The dissipation peaks in fact survive up to a temperature of about $T = 71 \pm 6\,\mathrm{K}$ (see Supplementary Fig. 4). As mentioned earlier, STM data show that short-range CDW order in $NbSe_2$ persists around surface defects or impurities at temperature up to $T = (2.5\text{–}3)T_{\mathrm{CDW}}$ (ref. 15). Up to that temperature, the tip potential itself may thus awaken a local CDW distortion, which can in turn exhibit similar dissipation phenomena to the long-range-ordered CDW.

To model and understand in detail the effect of the tip on the CDW, and ultimately the source of the dissipation peaks, we describe the density deformation as a simple elastic system interacting with an extended perturbation. Following well-established literature[21,22], we describe the CDW through phase and amplitude order parameters, the latter assumed constant for small perturbations. The overall density (ions and electrons) takes the form $\rho(x) = \rho_0 \cos(Qx + \phi(x))$, where Q is the wavenumber and ρ_0 the constant amplitude. The energy as a function of the order parameter $\phi(x)$ for an external perturbing tip potential $V(x)$ then reads:

$$E[\phi(x)] = \int [(\nabla\phi(x))^2 + V(x)\rho(x)]\,\mathrm{d}x \qquad (2)$$

To keep it simple, this description assumes a unidirectional CDW, but the same mechanism should hold in our tridirectional $NbSe_2$ experimental example. For a given external potential, the energy can be minimized to find the preferred phase shape along x. The main difference from previous treatments that were given for impurities[23] is that in this case, owing to the large size of the pendulum tip and swing, the potential $V(x)$ may extend over lengths longer than the characteristic CDW length scale $2\pi/Q \sim 2.5\,\mathrm{nm}$. This leads to new interesting effects. Further care needs to be taken in choosing the dimensionality of the system: although the relevant tip-related behaviour of the CDW is along x and restricted to the surface, a full treatment will have to take into account the other dimensions, namely y in the surface plane, and z into the underlying bulk, to obtain a realistic shape for the order parameter. These aspects will be discussed elsewhere, but here we will describe the effect in a simple one-dimensional model, which retains all of the necessary features without any of the complications connected with higher dimensionality.

An important role in understanding the dissipation mechanism is played by the boundary conditions: although we impose the phase to be fixed at the boundaries (consistently with an overall pinned CDW as known experimentally), this value is defined only modulo 2π. This leads to the existence of qualitatively different solutions of the energy minimization problem, where (along the main CDW direction) the perturbation may lead to a phase change $2\pi N$, with N being an integer, between the pinned boundaries. We call N

the 'winding number' of a given order parameter configuration. We minimize the energy in the subspace of one given winding number and observe its behaviour as a function of the perturbation amplitude, controlled by the tip position above the substrate. We show this energy in Fig. 3 for a perturbation of Lorentzian form $V(x;d)$, mimicking an approaching conical tip, as a function of the tip–sample distance d.

As energy curves for different winding numbers sharply cross at specific distances, marked by dashed circles, we expect the CDW phase winding number to switch from one N to the next $N \pm 1$ type of deformation at these points. Moreover, as shown in the inset (phase and density along the main CDW direction for different N), these solutions present a qualitative difference, akin to a symmetry difference, making a smooth transition between the two impossible. Passing through a crossover point will thus be accompanied by a hysteresis cycle in the tip mechanics, which explains the giant size of dissipation peaks despite the extremely low tip oscillation frequency as compared with the dielectric relaxation frequency (approximately megahertz) measured in a.c.-conductivity experiments[23]. To corroborate this picture, let us consider the height of the dissipation peaks it would produce, proportional to the area of the hysteresis cycle. We expect this area to be related to the angle between the energy curves α and the average slope at the crossing point β (see the blow up in Fig. 3). Considering that the area of the hysteresis cycle while oscillating around this point will behave like $W \propto \sin\alpha \cos^{-2}\beta$, we see from the shape of the $E(d)$ curves that the variation of these two parameters has opposite effects on the height of the peak as the tip approaches the surface, because a decreasing α would decrease the hysteresis area, whereas an increasing β would increase it. This provides a possible explanation of the non-monotonic peak intensity behaviour observed experimentally. A full treatment of the CDW-related dissipation materials should be followed by a more thorough theoretical treatment, which will be reported elsewhere. We can conclude here that the CDW phase slip model reproduces, at least qualitatively, the basic characteristics of the observed dissipation.

It is important before closing to make connection with earlier work, both experimental[20], where a single dissipation peak was reported on $NbSe_2$ and $SrTiO_3$, and theoretical[24], where a collective resonance of spin-like centres was ingeniously invoked to explain it. Our findings of a multiplicity of interaction force-controlled peaks in $NbSe_2$, and peaks systematically absent over NbS_2, suggest a different scenario. The train of peaks is perfectly reproducible and ubiquitous over well-ordered surfaces and clean $NbSe_2$ bulks, making the existence and nature of these centres doubtful (see Supplementary Fig. 5). The temperature evolution of the peaks suggests instead a strong connection with the CDW. A correspondence between each peak and the local pumping of a CDW phase slip is made especially compelling by theoretically finding a first-order energy crossing of states of the CDW with different winding numbers, implying the possibility of a mechanical hysteresis cycle even at the very low tip vibration frequency, where an alternative viscous dissipation could be barely detectable at best. In summary, we believe we identified a promising mechanism—coupling of a slider to a collective phase—that is new and deserves further experimental and theoretical study, extending to other systems with incommensurate bulk phases. It should apply in particular to genuine CDW and spin-density-wave materials, where the phase pumping should entail interesting surface flows of charge and spin under vibrating tips.

Methods

Sample. We used a high-quality 2H-$NbSe_2$ single-crystal sample of size $5 \times 5 \times 0.8$ mm^3 with a $T_{CDW} = 33$ K determined from temperature-dependent resistance measurements that is in agreement with previous results[25]. The crystal was produced by means of a standard chemical-vapour-transport technique with iodine as the transport agent[26]. The residuals were washed off the surface with solvents. The sample was cleaved under UHV conditions.

Pendulum AFM. The experimental set-up used for measuring friction at low temperature is described in detail in another publication[27]. Here we note that the probe consisted of a soft cantilever (ATEC-CONT from Nanosensors) with spring constant $k = 120$ mN m^{-1}. The probe was suspended perpendicularly to the surface with an accuracy of 1° and operated in the so-called pendulum geometry in which the tip vibrational motion is parallel to the sample surface. The oscillation amplitude $A = 5$ nm of the tip was kept constant using a Nanonis phase-locked loop feedback system. The cantilever tip is asymmetric as shown in Supplementary Fig. 1. Owing to this the perpendicular component of oscillation amplitude $A_{perp} = 180$ pm exists as well. The cantilever was annealed in UHV up to 700°C for 12 h, which results in the removal of water layers and other contaminants from both the cantilever and the tip. This is confirmed by the improvement of the quality factor of the probe by almost two orders of magnitude[28]. It is also known that this long-term annealing leads to negligible amounts of localized charges on the probing tip. After annealing, the cantilever was characterized by a resonance frequency $f = 12$ kHz and a quality factor $Q = 9 \times 10^5$. This led to the internal friction $\Gamma_0 = k/2\pi f_0 Q = 1.7 \times 10^{-12}$ kg s^{-1} and the corresponding dissipated power $P_0 = \pi k A^2/eQ = 65$ μW (at 6 K). The sample and cantilever temperatures were controlled by means of two different cryogenic controllers (Model 340 and Model DRC-91C from Lakeshore Cryotronics).

Tuning-fork-based STM/AFM. The STM/AFM experiments were performed with a commercial qPlus STM/AFM (Omicron Nanotechnology GmbH) running at low temperature (5 K) under UHV and operated by a Nanonis Control System from SPECS GmbH. We used a commercial tuning-fork sensor in the qPlus configuration (typical parameters: resonance frequency $f_0 \approx 25$ kHz, spring constant $k_0 \approx 1{,}800$ N m^{-1}, typical quality factor $Q = 35{,}000$ at 5 K). The oscillation amplitude was always set to 200 pm. The oscillation frequency $f(z)$ and excitation amplitude A_{exc} were recorded simultaneously for different V values applied to the tungsten tip. The force extraction was done by means of the Sader and Jarvis formula[19]. An additional $f(z)$ curve was taken (typical retraction distance ≈ 20 nm) after the complete spectroscopic measurement to estimate the long-range van der Waals background. All STM images were recorded in the constant-current mode.

Theoretical treatment. The energy $E[\phi(x)]$ given in equation (2) was minimized numerically through a simple conjugated gradient algorithm[29] on a two-dimensional discrete grid. The CDW was taken as unidirectional, whereas the other direction is required for a realistic minimization of the phase. Different boundary conditions were enforced to obtain solutions with different winding number N. Within the grid the gradient was considered modulo 2π to allow for phase jumps when $N \neq 0$. The external potential was taken as a Lorentzian depending on the tip–sample distance d as $V(r;d) = V_0(d)/(r^2 + \sigma(d)^2)$, with $V_0(d) \propto d^{-1}$ and $\sigma(d) \propto d^2$. This shape is found to be appropriate to model a conical tip interacting with the surface through van der Waals force. The parameters are estimated from a fit of the experimental overall tip–sample interaction within the same model.

Received 7 June 2013; accepted 12 November 2013; published online 15 December 2013

References

1. Urbakh, M. & Meyer, E. Nanotribology: The renaissance of friction. *Nature Mater.* **9,** 8–10 (2010).
2. Lantz, M. A., Wiesmann, D. & Gotsmann, B. Dynamic superlubricity and the elimination of wear on the nanoscale. *Nature Nanotech.* **4,** 586–591 (2009).
3. Socoliuc, A. *et al.* Atomic-scale control of friction by actuation of nanometer-sized contacts. *Science* **313,** 207–210 (2006).
4. Vanossi, A., Manini, N., Urbakh, M., Zapperi, S. & Tosatti, E. Modeling friction: From nanoscale to mesoscale. *Rev. Mod. Phys.* **85,** 529–552 (2013).
5. Kisiel, M. *et al.* Suppression of electronic friction on Nb films in the superconducting state. *Nature Mater.* **10,** 119–122 (2011).
6. Volokitin, A. I., Persson, B. N. J. & Ueba, H. Giant enhancement of noncontact friction between closely spaced bodies by dielectric films and two-dimensional systems. *J. Exp. Theor. Phys.* **104,** 96–110 (2007).
7. Stipe, B. C., Mamin, H. J., Stowe, T. D., Kenny, T. W. & Rugar, D. Noncontact friction and force fluctuations between closely spaced bodies. *Phys. Rev. Lett.* **87,** 096801 (2001).
8. Kuehn, S., Loring, R. F. & Marohn, J. A. Dielectric fluctuations and the origins of noncontact friction. *Phys. Rev. Lett.* **96,** 156103 (2006).
9. Wilson, J. A., Di Salvo, F. J. & Mahajan, S. Charge-density waves and superlattices in the metallic layered transition metal dichalcogenides. *Adv. Phys.* **24,** 117–201 (1975).
10. Moncton, D. E., Axe, J. D. & DiSalvo, F. J. Study of superlattice formation in 2*H*-$NbSe_2$ and 2*H*-$TaSe_2$ by neutron scattering. *Phys. Rev. Lett.* **34,** 734–737 (1975).

11. Inosov, D. S. *et al.* Fermi surface nesting in several transition metal dichalcogenides. *New J. Phys.* **10,** 125027 (2008).
12. Shen, D. W. *et al.* Primary role of the barely occupied states in the charge density wave formation of $NbSe_2$. *Phys. Rev. Lett.* **101,** 226406 (2008).
13. Borisenko, S. V. *et al.* Two energy gaps and Fermi-surface arcs in $NbSe_2$. *Phys. Rev. Lett.* **102,** 166402 (2009).
14. Weber, F. *et al.* Extended phonon collapse and the origin of the charge-density wave in 2H-$NbSe_2$. *Phys. Rev. Lett.* **107,** 107403 (2011).
15. Chockalingam, S. P. *et al.* Visualizing the charge density wave transition in 2H-$NbSe_2$ in real space. Preprint at http://arxiv.org/abs/1307.2282 [cond-mat.str-el] (2013).
16. Guillamón, I. *et al.* Superconducting density of states and vortex cores of 2H-NbS_2. *Phys. Rev. Lett.* **101,** 166407 (2008).
17. Soumyanarayanan, A. *et al.* Quantum phase transition from triangular to stripe charge order in $NbSe_2$. *Proc. Natl Acad. Sci. USA* **110,** 1623–1627 (2013).
18. Cleveland, J. P., Anczykowski, B., Schmid, A. E. & Elings, V. B. Energy dissipation in tapping-mode atomic force microscopy. *Appl. Phys. Lett.* **72,** 2613–2615 (1998).
19. Sader, J. E. & Jarvis, S. P. Accurate formulas for interaction force and energy in frequency modulation force spectroscopy. *Appl. Phys. Lett.* **84,** 1801–1803 (2004).
20. Saitoh, K., Hayashi, K., Shibayama, Y. & Shirahama, K. Gigantic maximum of nanoscale noncontact friction. *Phys. Rev. Lett.* **105,** 236103 (2010).
21. Fukuyama, H. & Lee, P. A. Dynamics of the charge-density wave. I. Impurity pinning in a single chain. *Phys. Rev. B* **17,** 535–541 (1978).
22. Lee, P. A. & Rice, T. M. Electric field depinning of charge density waves. *Phys. Rev. B* **19,** 3970–3980 (1979).
23. Tucker, J. R. Impurity pinning of sliding charge-density waves. *Phys. Rev. B* **40,** 5447–5459 (1989).
24. She, J-H. & Balatsky, A. V. Noncontact friction and relaxational dynamics of surface defects. *Phys. Rev. Lett.* **108,** 136101 (2012).
25. Li, L-J., Xu, Z-A., Shen, J-Q., Qiu, L-M. & Gan, Z-H. The effect of a charge-density wave transition on the transport properties of 2H-$NbSe_2$. *J. Phys. Conden. Matter* **17,** 493–498 (2005).
26. Kershaw, R., Vlasse, M. & Wold, Aaron The preparation of and electrical properties of niobium selenide and tungsten selenide. *Inorg. Chem.* **6,** 1599–1602 (1967).
27. Gysin, U., Rast, S., Kisiel, M., Werle, C. & Meyer, E. Low temperature ultrahigh vacuum noncontact atomic force microscope in the pendulum geometry. *Rev. Sci. Instrum.* **82,** 023705 (2011).
28. Rast, S. *et al.* Force microscopy experiments with ultrasensitive cantilevers. *Nanotechnology* **17,** 189–194 (2006).
29. Press, W. H., Teukolsky, S. A., Vetterling, W. T. & Flannery, B. P. *Numerical Recipes: The Art of Scientific Computing* 3rd edn (Cambridge Univ. Press, 2007).

Acknowledgements

F.P., G.E.S. and E.T. acknowledge research support by MIUR, through PRIN—2010LLKJBX_001, by SNSF, through SINERGIA Project CRSII2 136287/1, and by the EU-Japan Project LEMSUPER. E.T. acknowledges financial support from the ERC Advanced Research Grant No. 320796 MODPHYSFRICT. R.B. acknowledges financial support by the CNR program Short Term Mobility STM 2011. M.L., M.K., R.P., A.B. and E.M. acknowledge financial support from the Swiss National Science Foundation (NSF), the SINERGIA Project CRSII2 136287/1 and the Swiss National Center of Competence in Research on Nanoscale Science (NCCR-NANO). G.B. acknowledges financial support from EPSRC, UK(EP/I007210/1).

Author contributions

The samples were fabricated by G.B. The idea was born out of discussion between E.T., E.M., R.B., A.G., R.P. and M.K. The experiment was carried out by M.L., M.K. and R.P. R.B. and A.G. participated in sample preparation and the pendulum-AFM experiment. The theoretical model was developed by F.P., G.E.S. and E.T. E.T., E.M., A.B., F.P., G.E.S., R.B., A.G., M.L., M.K. and R.P. were involved in interpretation, discussion and paper writing.

Additional information

Supplementary information is available in the online version of the paper. Reprints and permissions information is available online at www.nature.com/reprints. Correspondence and requests for materials should be addressed to M.K.

Competing financial interests

The authors declare no competing financial interests.